



Comprehensive tissue homogenization and metabolite extraction for application in clinical metabolomics

Yuntao Hao^{a,b}, Jeannie Horak^{a,b,*}, Zorica Stijepic^{a,b}, Sultan Nilay Can^{a,b}, Luke Tu^{a,b}, Julia Alexandra Wolff^c, Berthold Koletzko^{a,b,**}

^a Department of Pediatrics, Dr. von Hauner Children's Hospital, LMU University Hospital, LMU Munich, Lindwurmstrasse 4, D-80337, Munich, Germany

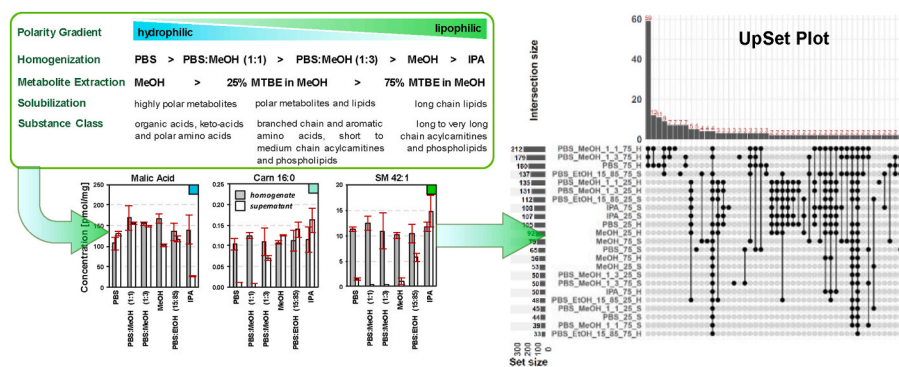
^b German Center for Child and Adolescent Health (DZKJ), site, Munich, Germany

^c Department of Medicine II, University Hospital, LMU Munich, Marchioninistrasse 15, 81377, Munich, Germany

HIGHLIGHTS

- Comprehensive broad range tissue homogenization and metabolite extraction.
- Comparison of six different homogenization solutions with increasing lipophilicity.
- Two-step metabolite and lipid extraction using MeOH and 75 % MTBE in MeOH.
- Prewetting correction factor for homogenates with high solid content.
- Upset Plot with 75 % concentration threshold for extraction efficiency comparison.

GRAPHICAL ABSTRACT



ARTICLE INFO

Keywords:

Tissue homogenization
Homogenate
Prewetting
Metabolomics
Lipidomics
HPLC-ESI-QTRAP-MS/MS
Upset plot

ABSTRACT

Background: Metabolomics and lipidomics analysis of various biological samples offer insights into potential mechanisms of health and disease development. Tissue samples, compared to other biological samples, are less elucidated due to challenges in sample collection and lack of standardized sample preparation protocols for reproducible tissue homogenization and broad-range metabolite extraction.

Results: Pork tissue samples were homogenized with six different solvent mixtures with increasing lipophilicity, followed by metabolites extraction using methanol for polar and methyl-*tert*-butyl ether (MTBE) in methanol (MeOH) for highly lipophilic compounds. Metabolite profiles of supernatant and homogenate extraction for three extract volumes were compared. Solvent dependent pipette tip blockage was addressed by introduction of a prewetting correction factor for non-polar homogenization solutions and low volume tissue homogenate pipetting. Upset plots were applied for multi-dimensional metabolite extraction efficiency evaluation for 24 different sample preparation conditions. The best-performing homogenization solution was PBS; MeOH (1:1; v/v),

* Corresponding author. Department of Pediatrics, Dr. von Hauner Children's Hospital, LMU University Hospital, LMU Munich, Lindwurmstrasse 4, D-80337, Munich, Germany.

** Corresponding author. Department of Pediatrics, Dr. von Hauner Children's Hospital, LMU University Hospital, LMU Munich, Lindwurmstrasse 4, D-80337, Munich, Germany.

E-mail addresses: Jeannie.Horak@med.uni-muenchen.de (J. Horak), Berthold.Koletzko@med.uni-muenchen.de, office.koletzko@med.lmu.de (B. Koletzko).

<https://doi.org/10.1016/j.aca.2025.343728>

Received 18 October 2024; Received in revised form 22 January 2025; Accepted 24 January 2025

Available online 25 January 2025

0003-2670/© 2025 The Authors. Published by Elsevier B.V. This is an open access article under the CC BY license (<http://creativecommons.org/licenses/by/4.0/>).

combined with a two-step polar metabolite and lipid extraction using MeOH and 75 % MTBE in MeOH employing the tissue homogenate. The optimized experimental conditions were applied on mouse pancreas tissues, providing evidence of varying metabolic pathway activities across different anatomical regions of an organ.

Significance: This study introduces a comprehensive tissue sample preparation and metabolite quantification workflow, covering highly polar to highly lipophilic metabolites using targeted high performance liquid chromatography electrospray ionization triple quadrupole-linear ion trap mass spectrometer (HPLC-ESI-QTRAP-MS/MS) for absolute quantitation of amino acids, organic acids and keto-acids, acyl-carnitines, and phospho-choline lipids.

1. Introduction

In biomedical research, comprehensive and reproducible cell and tissue homogenization is an essential sample preparation step prior to analyte extraction. Since tissue samples of various organs and muscle types enclose a large amount of highly diverse information, ranging from DNA [1], RNA [2], proteins [3], lipids [4], and polar metabolites [5], their respective sample preparation protocols vary accordingly. Besides the ultrasonic homogenization technique [6] as well as classic tissue homogenization approaches using pestle [7,8], Dounce homogenizer [2,8], ultra-turrax [3], mortar [9] and ball mill [10], bead-based homogenization [8,11] has gained increased attraction due to its applicability for high-throughput sample preparation. While single sample homogenizations are sufficient in biology and biochemical research, in clinical research and especially in clinical routine analysis large-scale sample preparations performed in parallel are not only time saving, but also enhances the overall sample-to-sample reproducibility by employing automation and sample cooling during homogenization, e.g. Pycellys [11], Quiagen [8], Bullet Blender [8] and Beadbug [12]. Alternatively, a homemade set screw homogenizer [8] can be used, but this device does not allow sample cooling.

It is rather difficult to directly compare results obtained with different sample preparation protocols due to marked variations in tissue homogenization protocols employing not only different types of homogenization tools, but also major differences in the choice of homogenization and analyte extraction solutions. For instance, using a pestle will break open cells to gain access to the cell content using shear force, but will not necessarily also crush organelles, cell nuclei, and lipid membranes. On the other hand, a steel bead-based tissue homogenizer is even powerful enough to homogenize bones [13], which makes this method superior to other state-of-the-art tissue homogenization strategies, since it can crush all types of biological matrices down to their smallest cell compartment, the organelles and their lipid membranes. Alternatively, a newly introduced, low cost, mild and easy to implement metabolite from tissue extraction technique employs solid phase microextraction (SPME) to capture intracellular metabolites from tissue without extraction of membrane lipids [12].

Most sample preparations were originally optimized for single substance classes and hence do not cover other compound groups, for which another protocol utilizing an additional tissue sample must be used. In the case of tissue biopsy samples, such as brain or tumor tissue, it would be of great advantage to be able to gain as much information as possible from small, single tissue pieces. Modern technology already allows real-time mass spectrometric tissue evaluation directly in the operating theater using integrated rapid evaporative ionization mass spectrometry (REIMS) with the Harmonic scalpel also known as an intelligent knife (iKnife) [14,15] as well as tissue imaging mass spectrometry [16] and spatial multi-omics technology [17] of tissue biopsy sections. However, the instruments involved are not only costly but also highly specialized. In clinical metabolomics, cost-effective high sample throughput is only feasible with automation of as many sample-preparation steps as possible, including analyte extraction and derivatization [18]. This approach can only be realized by utilizing 96-well plates instead of single 15 mL glass tubes and by replacing two-phase extraction

procedures such as Bligh and Dyer [19] for lipid extraction with one-phase solvent extraction methods [20]. Overall, it was found that combining tissue homogenization with multiple solid-liquid metabolite extraction steps using solvents with increasing lipophilicity will significantly increase metabolite and lipid coverage [7,12,21]. Nonetheless, if more than two extraction steps are employed, the sample preparation process becomes lengthy and laborious, especially if homogenization is performed individually using a pestle [7] instead of utilizing a multi tube bead homogenizer [12]. An often-neglected factor is the difference in metabolic profiles between the supernatant, tissue homogenate slurry, and the tissue debris pellet after supernatant removal. A recent study demonstrated that homogenate slurry and tissue debris pellet contained many lipids when homogenization solvents with high water content were used, while for non-aqueous organic solvent methanol, the lipid content is practically identical for homogenate and supernatant [9]. Nonetheless, the most common approach is to employ the supernatant for metabolite and lipid extraction [21–23], and only in recent years the application of the homogenate is discussed [9,24]. Also, the choice of homogenization solvent and solvent mixtures as well as recommended tissue weight to homogenization solvent volume ratios varied not only between different research facilities but also for different tissue types [21,22]. Different extraction methods used to extract metabolites from the same homogenate slurry will lead to different metabolic profiles [25]. In addition, the presence or absence of additional cooling during tissue homogenization will influence metabolite and lipid composition, due to temperature-induced chemical and enzymatic conversion and degradation processes [26–29]. Pipetting of a homogenate slurry can be challenging, since the number of solids increases with increasing organic solvent content, which can lead to severe pipette tip blockage.

The present research study aims to compare the influence of solvent polarity on bead-based tissue homogenization and metabolite extraction efficiencies for polar to highly lipophilic metabolites employing solvent mixtures with increasing lipophilicity. In this context, six different homogenization solutions (PBS, PBS:MeOH (1:1), PBS:MeOH (1:3), PBS:EtOH (15:85) and IPA) and three different metabolite extraction solutions (MeOH, 25 % MTBE in MeOH and 75 % MTBE in MeOH) in a two-step extraction approach for supernatant as well as homogenate have been investigated. In addition, three different homogenization extract volumes (10 μ L, 25 μ L and 50 μ L) are compared and a pipette tip pre-wetting correction factor is introduced for accurate pipetting of tissue homogenates of lipophilic organic solvents such as isopropanol using small pipette tips (10 μ L), which are prone to pipette tip blockage and hence require a prewetting step. Besides that, also an easy implementable ice-bag cooling for the Bead Ruptor 4 homogenizer is introduced. For convenience, all method development experiments are conducted with commercial pork tissue, but the best performing condition is then applied to a small set of mouse pancreatic tissue samples. As expected, there are a multitude of influential factors in play as well as several possible pitfalls to consider, especially when performing tissue homogenization combined with the overall goal to comprehensively extract highly polar as well as lipophilic metabolites. The current study aims to characterize some of the most influential sample preparation factors in tissue metabolomics, and to provide feasible solutions to the problems

encountered.

2. Materials and methods

2.1. Chemicals and consumables

LC-MS grade water, methanol (MeOH), acetonitrile (ACN) and isopropanol (IPA), and LC-grade ethanol (EtOH), as well as methyl *tert*-butyl ether (MTBE), phosphate buffer saline (PBS) from Gibco, 200 μ L PCR 96-well microplates (conical, skirted) from Axygen and 1.2 mL 96 deep-well plates (round bottom, low profile) from Brand, were purchased from Sigma-Aldrich (Schnelldorf, Germany). ClinChek human control plasma (Level I and II) from Recipe (Munich, Germany) was used as pooled quality controls (QCs) and as individual control plasmas (CPI and CPII). A detailed list of standards and internal standards, including their abbreviations is provided in the Supporting Information. TipONE 10 μ L, 200 μ L, and 1000 μ L pipette tips were purchased from StarLab (Hamburg, Germany). The PCR microplate aluminum heat sealing foil, the Multipette M4, the HeatSealer S100, and the ThermoMixer C with well plate adapter were from Eppendorf (Wesseling, Germany). Polypropylene PCR microplate foil was from RatioLab (Dreieichen, Germany). The tungsten carbide 3 mm beads were from QIAGEN (Hilden, Germany). The 2 mL screw cap tubes were from Sarstedt (Nümbrecht, Germany). The reinforced 2 mL screw caps with caps for tissue homogenization and the Bead Ruptor-4 tissue homogenizer (with adjustable intensity levels 1 to 5 with 5 being the highest) were from Omni-International, both were purchased from Biolabproducts GmbH (Bebensee, Germany). The digital food thermometer HCPI was from Habor (Taiping City, Taiwan). The analytical balance PRACTUM64-1S (0.1 mg–1 g) was from Sartorius Lab Instruments GmbH & Co. KG (Goettingen, Germany). The vortexer was from IKA®-Werke GmbH & Co. KG (Staufen, Germany). Centrifuges MIKRO 22 R and ROTINA 380 R Hettich centrifuge (for well plates) are from Andreas Hettich GmbH & Co. KG (Tuttlingen, Germany). The nitrogen generator NGM 22-LC/MS was from CMC Instruments GmbH (Eschborn, Germany). The nitrogen sample concentrator with Dri-Block DB100/3 heater, sample concentrator, PTFE coated needles and 96-well block thermostat for Dri-block were from Techne, purchased from VWR (Darmstadt, Germany).

2.2. Tissue sample preparation

2.2.1. Preparation of pork tissue samples

The pork chops were purchased from a local supermarket within a warranty period. The pork tissue was rinsed with sterile PBS solution and cut with a disposable scalpel on a clean glass plate into 100 mg \pm 10 mg pieces, which were directly weighed ($n = 4$) into 2 mL screw cap tubes with reinforced caps. All tissue samples were shock-frozen for 10–20 s in liquid nitrogen before storage at -80 °C before homogenization.

2.2.2. Preparation of mouse pancreas tissue samples

The mouse pancreas samples were provided by Julia Alexandra Wolff (University Hospital, LMU Munich). Female C57BL6/J mice on a standard diet and under normal housing conditions were sacrificed according to §4 of the German Animal Welfare Act (Tierschutzgesetz) for scientific investigations. The pancreas of three mice, one at 17 weeks of age ($M - 1$) and two mice at 15 weeks of age ($M - 2$ and $M - 3$), was randomly divided into 3 tissue pieces (A, B, and C) of similar weight (50 mg \pm 10 mg). Each piece of pancreas tissue was weighed ($n = 3$) according to the above stated procedure in 2 mL tubes with reinforced screw caps for later homogenization. Tissue was snap-frozen in liquid nitrogen and stored at -80 °C before homogenization.

2.3. Tissue homogenization

2.3.1. Temperature control during tissue homogenization

The Bead Ruptor-4 tissue homogenizer can only process 4 tubes simultaneously without cooling. To each pork tissue sample tube, five 3 mm steel beads and 300 μ L of PBS were added. The temperature of the homogenization solution in the respective tube as well as that of the homogenate was determined with a digital food thermometer before (0 min) and after homogenization at intensity level 4 for different time periods (30 s–5 min) and under different cooling regimes. If not otherwise specified, in-solution temperature was measured only once, since it rapidly increased within seconds.

Experiment 1: A single homogenization tube was placed in liquid nitrogen (-196 °C) for 20 s before each successive test run with 1, 2-, 3-, 4- and 5-min duration times (Fig. 1a). The same test tube was frozen at the beginning of each test run. The in-solution temperature was measured four times in a row for standard deviation calculation.

Experiment 2: One homogenization tube was placed on crushed ice for pre-cooling and two samples were cooled at -20 °C for 5 min followed by homogenization for 30 s. One of the two -20 °C cooled samples were additionally cooled by placing a zip-lock bag filled with crushed ice and a little water under the homogenizer lid (Fig. S1a).

Experiment 3: A single homogenization tube was repeatedly cooled at -20 °C for 5 min before successive homogenization for 0.5, 1.0 and 1.5 min, placing the zip-lock bag with crushed ice i) under the homogenizer lid and ii) on top of the lid (Fig. S1b). The in-solution temperature was measured before and after homogenization.

Experiment 4: A single homogenization sample tube was cooled at -20 °C for 5 min before successive homogenization for 0.5, 1.5, 3 and 5 min, placing the zip-lock bag with crushed ice between the sample tubes and the homogenizer lid (Fig. 1b)

2.3.2. Influence of homogenization solvent polarity

To each pork tissue sample tube (100 mg; $n = 4$), five 3 mm steel beads and 300 μ L of the corresponding homogenization solution, namely PBS, PBS/MeOH (1:1; v/v), PBS/MeOH (1:3; v/v), PBS/EtOH (15:85; v/v), MeOH and IPA, were added. Tissue homogenization was performed at homogenization level 4 for 5 min using a zip-lock bag with crushed ice, placed under the Bead Ruptor 4 lid for cooling. All homogenate

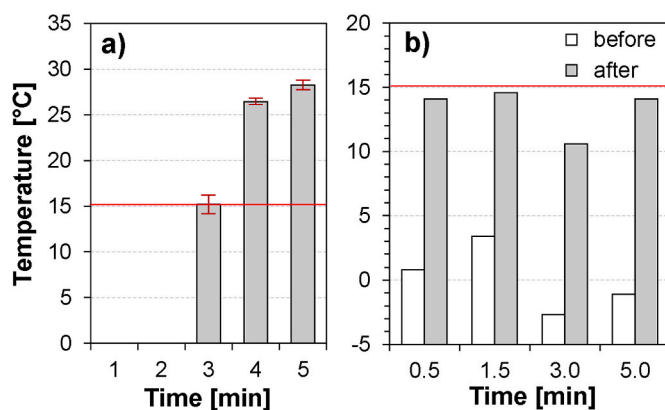


Fig. 1. Tissue homogenization was performed in PBS at intensity level 4 using 5×3 mm steel beads. For experiments shown in a), the homogenization tubes ($n = 3$) were kept in liquid nitrogen for 20 s and homogenization was performed subsequently in 1 min intervals at room temperature, while in b) the homogenization tube ($n = 1$) was cooled for 5 min. at -20 °C followed by homogenization using crushed ice between the sample and homogenizer lid for continuous sample cooling. In-solution temperature was measured before and after homogenization. The red line indicates the propounded maximum threshold of 15 °C homogenate temperature. (For interpretation of the references to colour in this figure legend, the reader is referred to the Web version of this article.)

tubes were kept on ice before and after homogenization as well as before and after metabolite extraction. Note that none of the homogenates were re-frozen and that metabolite extraction was performed immediately after homogenization. Metabolite and lipid extraction was performed subsequently for three different homogenate and supernatant volumes (10 μL , 25 μL , and 50 μL) for both two-step extraction processes, i) MeOH and 25 % MTBE in MeOH and ii) MeOH and 75 % MTBE in MeOH. In both cases, the internal standard (ISTD) mixture was added to the first extraction solvent. Note that homogenate extraction was performed before centrifugation and supernatant extraction for the same homogenization samples.

2.3.3. Investigation of possible background contamination

Three different background contamination checks were performed in quadruplets. For **Blank 1**, four empty tubes were filled with five 3 mm steel beads and 300 μL of the respective homogenization solution. Homogenization was performed in parallel with the pork tissue samples, employing the two-step metabolite extraction procedure with 25 % and 75 % MTBE in MeOH in the second step.

For **Blank 2** the respective homogenization solution underwent the two-step metabolite extraction process without the homogenization step. In the case of **Blank 3**, the respective homogenization solution was directly pipetted into the methanolic ISTD solution and analyzed without any pre-processing, except the required LC-MS-related sample preparation steps. Note that **Blank 2** is equivalent to the commonly co-analyzed ISTD-blank or zero-blank.

2.4. Extraction of polar and non-polar metabolites

2.4.1. Extraction of polar metabolites

Using a Multipipette M4 stepper pipette, 450 μL of the methanolic ISTD mix solution (ISTD) was pipetted into the designated wells of the 1.2 mL 96-deep-well plate (well plate A). After pipetting 10 μL , 25 μL and 50 μL of the vortexed homogenate slurry (4x for each volume) as well as 50 μL QC plasma (6x), 50 μL CPI (2x), 50 μL CPII (2x) and 50 μL water (1x) for the ISTD blank, directly into the respective ISTD solutions by draw and eject (20x) with the pipette tip, a homogenous protein precipitate is formed for both, the tissue homogenate and the plasma samples (QC and CP). The homogenate tubes were then centrifuged for 10 min at 10000 rcf and 4 $^{\circ}\text{C}$. From the respective tissue homogenate supernatants ($n = 4$), 10 μL , 25 μL and 50 μL of the clear extracts were carefully pipetted into the ISTD solution without elutriation of the homogenate solids. Note that 10 μL extract volume was excluded for the 75 % MTBE in MeOH extraction experiments. The metabolite extraction well plates were covered with PCR foil and shaken for 20 min at 700 rpm and 25 $^{\circ}\text{C}$, before placing them in the refrigerator at 4 $^{\circ}\text{C}$ for 20 min to complete the protein precipitation process. The well plates were then centrifuged at 3000 rpm for 5 min at 22 $^{\circ}\text{C}$. The polar metabolite extract A was transferred to new 1.2 mL 96-well plates (well plate B; Fig. 2).

2.4.2. Extraction of lipids using 25 % and 75 % MTBE in methanol

The protein pellet in well plate A was immediately resuspended with 50 μL water by shaking the 96-well plate for 20 min at 800 rpm and 25 $^{\circ}\text{C}$. The protein slurry was precipitated by adding 450 μL 25 % MTBE (or 75 % MTBE) in MeOH, followed by drawing and ejecting with the pipette tip (20x) to obtain a flocculent precipitate. The well plate was shaken, incubated at 4 $^{\circ}\text{C}$, and centrifuged as previously described for polar metabolites. The supernatant was combined with the polar metabolite extract in well plate B (Fig. 2).

Immediately afterwards, 600 μL of the pooled extract was transferred into a new 1.2 mL well plate (well plate C1), while the residual 400 μL of pooled MTBE-containing extract remained in well plate B (= wellplate C2 in Fig. 2), which was covered with PCR foil before storage at -30°C before lipidomics analysis (phosphocholines and acylcarnitine). The pooled extract in well plate C1 (Fig. 2) was evaporated to dryness using a gentle stream of nitrogen at 25 $^{\circ}\text{C}$ and was redissolved in 300 μL 10 %

Tissue Homogenization

- 2 mL Screw cap tube with 3 mm steel beads (5x)
- 100 mg Pork tissue with 300 μL homogenization solution
- Homogenize for 5 min at level 4
- Ice bag cooling between lid and tube



Addition of Internal Standard + Protein precipitation + Extraction of polar metabolites and lipids

- 1) Pipette 50 μL (optionally 25 μL or 10 μL) of tissue homogenate (or supernatant after centrifugation) into 450 μL of ISTD in MeOH in well plate A to extract polar metabolites.

Centrifuge protein pellet and transfer the polar extract to a new well plate B

- 2) Add 50 μL water to resuspend the protein pellet in well plate A and add 450 μL 75% (or 25%) MTBE in MeOH to extract lipids.

Centrifuge the protein pellet and transfer the lipophilic extract to well plate B.

- 3) Split the pooled extract to well plates C1 (600 μL ; concentrate to 300 μL) and C2 (400 μL ; use as is) for polar metabolite and lipid analysis.

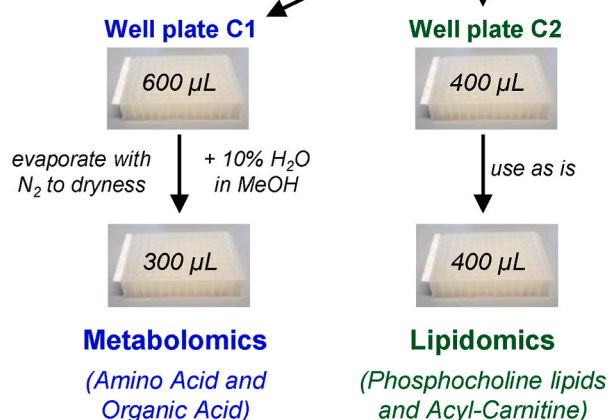


Fig. 2. Workflow for tissue homogenization, followed by polar metabolite extraction (well plate A) using methanol (containing ISTD mix) and medium to non-polar lipid extraction using optionally 25 % or 75 % MTBE in methanol. After pooling both extracts (well plate B), 400 μL of this extract pool was directly used for lipidomics analysis (well plate C2), while the remaining 600 μL extract was evaporated to dryness and reconstituted in 300 μL 10 % water in methanol for metabolomics analysis (well plate C1).

water in MeOH, which resembled a 1:1 concentration step. Well plate C1 was covered with PCR foil and stored at -30°C before polar metabolite analysis (amino acids and organic acids). Note that polar metabolite and lipid extracts were kept at -30°C for short term storage (a few days) and at -80°C for long term storage (weeks or month) before sample preparation for UHPLC-ESI-QTRAP-MS/MS analysis for amino acid [26], organic acid and keto-acid [30], acylcarnitine [10] and phosphocholine lipid analysis [31].

2.5. Volume correction for homogenate pipetting with pipette tip prewetting

For the determination of the volume correction factor for pipetting of tissue homogenates using pipette tip prewetting, empty pipette tips (A), pipette tips with residual homogenate slurry (RHS) after prewetting and ejection of the homogenate (B), pipette tips filled with homogenate without prewetting (C) and pipette tips filled with homogenate after prewetting (D) were weighed ($n = 5$ each). Prewetting was performed by multiple draw-and-eject cycles before the homogenate was pipetted. The pipette tips tested were 10 μL and 200 μL TipONE tips from StarLab. The pipetting volumes tested were 10 μL , 25 μL , and 50 μL . Only for homogenization solutions with a high percentage of organic solvent a prewetting correction factor (PWC-factor) was calculated since the purely aqueous PBS and the 50 % MeOH in PBS solutions did not induce pipette tip blockage and could be pipetted without prewetting (Table S1).

The weight of the residual homogenate slurry (RHS) was determined using two different equations (Eq. (1) and Eq. (3)). In addition, the calculated pipetting volume (PV) employing prewetting (Eq. (2)) is compared with the weighted correct pipetting volume without prewetting (Eq. (4)) and the weighted incorrect pipetting volume after prewetting (Eq. (5)).

The PWC-factor in % was calculated using Eq. (6) and Eq. (7) (Table S2 and Table S3). For volume correction, PWC-factor₂ was employed using Eq. (8).

$$\text{RHS}_1 = B - A \quad (\text{Eq. 1})$$

$$\text{PV}_1 = D - B \quad (\text{Eq. 2})$$

$$\text{RHS}_2 = D - C \quad (\text{Eq. 3})$$

$$\text{PV}_2 = C - A \quad (\text{Eq. 4})$$

$$\text{PV} + \text{RHS} = D - A \quad (\text{Eq. 5})$$

$$\text{PWC-factor}_1 = (B - A) \times 100 / (D - A) \quad (\text{Eq. 6})$$

$$\text{PWC-factor}_2 = (D - C) \times 100 / (D - A) \quad (\text{Eq. 7})$$

$$\text{Concentration (corrected)} = \text{Concentration (original)} \times (1 - \text{PWC-factor}_2 / 100) \quad (\text{Eq. 8})$$

2.6. Mouse pancreas tissue sample preparation

To each mouse pancreas sample tube (50 mg \pm 10 mg; $n = 1$), five 3 mm steel beads and 300 μL PBS/MeOH (1:1; v/v) were added for tissue homogenization at level 4 for 5 min using a zip-lock bag with crushed ice for cooling. For metabolite and lipid extraction, 50 μL of homogenate ($n = 4$) without pipette tip pre-wetting was used in combination with the two-step extraction procedure employing MeOH (plus ISTD) and 75 % MTBE in MeOH. Metabolomics profiling was performed as described for pork tissue.

2.7. Instrumentation and methods

The targeted HPLC-ESI-QTRAP-MS/MS analysis of 20 proteinogenic amino acids plus ornithine (Orn) and citrulline (Cit) was performed on an Agilent 1100 HPLC system comprised of a binary pump (G1312A), a degasser (G1379A), a well plate autosampler for 2 well plates (G1367A), 1290 thermostat (G1330B) and column oven (G1316A) from Agilent Technologies, Inc. (Waldbronn, Germany) coupled to the triple quadrupole (QqQ) API 2000 with electrospray ionization source (ESI) from AB SCIEX Pte. Ltd. (Concord, Canada). Chromatographic separation was performed on an XBridge C18 column (2.1 mm \times 150 mm, 3.5 μm) from Waters GmbH (Eschborn, Germany) [32,33]. For the targeted organic acid, keto-acid and lipid analysis, an Agilent 1260 HPLC system with binary pump (G1312B), a degasser (G1379B) and a 1260 multi-sampler

for 8 well plates (G7167A) from Agilent Technologies, Inc. (Waldbronn, Germany) combined with MayLab column oven for up to six columns from MayLab (Vienna, Austria) was used. This HPLC system was coupled to a hybrid QTRAP 4000 with ESI source from AB SCIEX Pte. Ltd. (Concord, Canada). Organic acids and keto acids (15) were separated on a Kinetex F5 column (2.1 mm \times 150 mm, 2.6 μm) from Phenomenex (Aschaffenburg, Germany) [30]. Acylcarnitines (60) were separated on a Kinetex EVO C18 column (2.1 \times 150 mm, 2.6 μm) from Phenomenex (Aschaffenburg, Germany) [34,35]. Phosphocholine lipids (PCaa, PCae, LPCa, LPCe, and SM; for acyl and e for ether) were analyzed in flow-injection-analysis (FIA) mode without column [36]. A detailed description of each metabolomics platform analysis including list of standards, internal standards and LC-MS/MS parameters is provided in the Supporting Information.

2.8. Software information and statistical data evaluation

Analyst 1.6.1 for data acquisition and MultiQuant™ 3.0.3 for quantitative data analysis were from SCIEX (Concord, Canada). Quantitative metabolite results were converted from $\mu\text{mol/L}$ to pmol/mg tissue, taking the individual tissue weight, pipetting volume, and if required, also the PWC-factor 2 into account. For data visualization, the R statistical software (version 4.1.0) in combination with the R-packages UpsetR [37], ComplexUpset [38], dplyr, ggplot2, tidyr and scales, as well as MS Office Excel were used. For automated peak integration, isotopic correction, and quantification of phosphatidylcholine lipids an in-house developed R-script was employed. For Upset plot generation, the entire data set for 50 μL volume of homogenate (H) and supernatant (S) for both metabolite extraction methods employing 25 % and 75 % MTBE in MeOH in the second extraction step were used. For extraction efficiency comparison, a 75 % concentration threshold for the highest concentrated metabolite for each metabolite from the full data set comprising the results for all sample preparation conditions using 50 μL extract volume, was applied. In order to visually simplify the Upset plots, an intersection size threshold of <2 was introduced. For comparison, an Upset plot generated with a 75 % concentration threshold for the best performing sample preparation condition (PBS:MeOH (1:1, v/v) for tissue homogenization combined with 75 % MTBE in MeOH in the second extraction step employing the homogenate) was used to compare this condition to the extraction efficiency of all other sample preparation conditions (Fig. S3). For a better understanding of Upset plots, a detailed comparison between Venn diagram and Upset plot is provided in the Supporting Information.

3. Results and discussion

3.1. Temperature controlled tissue homogenization

Although the BeadRuptor 4 tissue homogenization device is powerful and highly efficient, a major drawback is the absence of cooling during tissue homogenization. The measured temperature increases during tissue homogenization using 5 \times 3 mm steel beads per homogenization tube was 15 $^{\circ}\text{C}$ per minute higher than expected, reaching temperatures of almost 30 $^{\circ}\text{C}$ within 3 min (Fig. 1a) upon thawing. The general aim was to find a suitable cooling strategy to keep the homogenate temperature below 15 $^{\circ}\text{C}$ throughout a 5-min homogenization process. This 5 min homogenization time at intensity level 4 was chosen prospectively for its ability to also process tough biological material, without the need for re-optimization for other sample types at a later point in time. However, the 15 $^{\circ}\text{C}$ temperature threshold level was selected, because it could easily be adhered. It was found that freezing the tissue samples with the steel beads and the homogenization solution at -196°C with liquid nitrogen led to a processing time loss of 2 min, during which the sample remained frozen. Once thawed, there was an immediate 15 $^{\circ}\text{C}$ temperature jump within 1-minute (Fig. 1a). Keeping the thawed sample on crushed ice or at -20°C for 5 min before

homogenization leads to a temperature increase to 28 °C and 20 °C within 30 s (Fig. S1a). Comparing sample cooling with a zip-lock bag filled with crushed ice placed on the lid and under the homogenizer lid (Fig. S1b) provided best results for the latter, for which an in-solution temperature of uniformity 12–15 °C for the homogenate could be kept (Fig. 1b). For all following tissue homogenization experiments, 5 min processing time after 5 min pre-cooling at –20 °C and icebag cooling during homogenization were employed.

3.2. Prewetting correction factor for homogenate slurry pipetting

Depending on the homogenization solvent and solvent mixtures used as well as which type of pipette tip (10 µL or 200 µL) was employed, the homogenate can be easily pipetted without prewetting (accurate volume) or a prewetting by draw and eject of the homogenate slurry was indispensable due to tip blockage. It was observed that with increasing organic solvent content in the homogenate solution and decreasing pipette tip size, the frequency of pipette tip blockage increased (Table 1). For all experiments, where pipette tip pre-wetting was indispensable (Table S1), a new volume correction factor, which we named prewetting correction factor (PWC-factor) was introduced, since the remaining homogenate slurry in the pipette tip can lead to a 10 %–20 % higher pipetted volume for prewetting compared to without. For all homogenate solutions pipetted with prewetting, the PWC-factor₂ (Table 1) calculated with Eq. (7) was used. Since our established first-step sample preparation procedure (Fig. 2) includes the pipetting of a biological sample directly into the methanolic ISTD solution, correct volume pipetting is essential. The PWC-factor₂ in Table 1 was determined for four different homogenization solutions, two different pipette tip sizes (10 µL and 200 µL) and three different homogenate volumes (10 µL, 25 µL and 50 µL; n = 5 tips with n = 5 weighing each).

For comparison, Table S2 provides the PWC-factor₁ (Eq. (6)) results and Table S3 the results for single experiments and quintuplet weighing for all homogenization solutions. Unfortunately, additional homogenization for 1–2 min does not decrease the particle size of solids in the homogenate. Considering that the size and volume of solids in the homogenate increases with increased organic solvent content in the homogenization solution and considering that proteins in biological sampler precipitate in organic solvents, it can be assumed that these solids are a complex mixture of cell debris and protein precipitate. Once these solids are centrifuged and stored at low temperatures over a certain period, it is impossible to disperse the obtained cell debris-protein pellet back into a homogenous flocculent slurry. Therefore, metabolite and lipid extraction must be performed shortly after tissue homogenization, on the same day.

Table 1

Frequency of pipette tip blockage due to solids in the homogenate (x-out-of-10) and PWC-factor₂ (for n = 5 with n = 5 weighing).

	Tip Blockage Frequency			PWC-Factor ₂ [%]		
	10	200	200	10	200	200
Pipette Tip Size [µL]	10	200	200	10	200	200
Pipetted Volume [µL]	10	25	50	10	25	50
PBS:MeOH (1:1)	2*	0	0	0*	0	0
PBS:MeOH (1:3)	6	0	1*	14.62 ± 4.24	0	0*
MeOH	5	0	1*	15.62 ± 6.26	0	0*
PBS:EtOH (15:85)	8	4	6	15.20 ± 5.39	10.40 ± 2.62	10.72 ± 0.79
IPA	9	7	8	14.59 ± 8.31	10.69 ± 3.31	11.25 ± 1.39

For PBS no pipette tip blockage was observed and for frequencies below 3 (*), experiments were repeated with a fresh pipette tip without prewetting.

3.3. Homogenization solution and extract volume selection

The measured metabolites were divided into substance classes with decreasing polarity and increasing lipophilicity in the order of organic acids, amino acids, acylcarnitines, lyso-phosphatidylcholines (Lyso-PCs), phosphatidylcholines (PCs) and sphingomyelins (SMs). In addition, compound lipophilicity increases within a substance group with increasing alkyl-chain length, as shown in in Fig. 3 for acylcarnitines (Carn 4:0 < Carn 9:0 < Carn 16:0) and phospholipids (LPC < LPC 24:0; PC 18:2 < PC 38:0; SM 26:4 < 42:1). Also, the contribution of additional polar functional groups with increasing polarity such as hydroxy (OH) and carboxylic acid (DC) were considered, as illustrated in Fig. 3 for acylcarnitines (Carn 4:0 < Carn 4:0 OH < Carn 4:0 DC). If not otherwise stated, LPC and PC compounds are of the mono- and di-acyl type (LPCa and PCaa; for acyl). Their mono-alkyl and acyl-alkyl variants (LPCe and PCae; e for ether) have been analyzed, but will not be discussed in detail. Due to the large data set, encompassing 401 metabolites, metabolite profile changes in dependency of homogenate solution polarity, extract type (homogenate or supernatant), extract volume (10 µL, 25 µL, and 50 µL), and lipid extraction solution (25 % MTBE and 75 % MTBE) will be displayed only for selected metabolites. All metabolite concentrations are converted from µmol/L to pmol/mg tissue taking pipette tip prewetting, pipetted extract volume, and exact tissue weight into account.

To better visualize and compare extraction efficiencies, a normalization to 50 µL extraction volume has been applied for Fig. S2, while for Fig. 3 only 50 µL homogenate and supernatant results are illustrated. In all cases, a consistent tissue weight (100 mg) to homogenization solution volume (300 µL) ratio of 1-to-3 is employed. The investigated homogenization solutions cover a wide polarity range: PBS, PBS:MeOH (1:1), PBS:MeOH (1:3), PBS:EtOH (15:85), MeOH and IPA. Note that PBS:EtOH (15:85) and IPA are literature-recommended homogenization solutions to be used in combination with the Biocrates metabolomics and lipidomics kits [31] and are therefore placed side-by-side in Fig. 3 and Fig. S2. In general, homogenate slurries were more difficult to pipette for small volumes with high organic solvent content, which got worse with increasing solvent lipophilicity. However, employing the homogenate slurry provides more consistent and comparable results for 25 µL and 50 µL homogenate compared to their respective supernatants and are also less homogenization solution type dependent. Especially, for long-chain lipids such as SM 42:1 (Fig. 3), aqueous solutions with low organic solvent content reduce the overall extraction efficiency from supernatant significantly, while employing the homogenate leads to reproducible quantitative results, which are mostly independent of the homogenization solution and extract volume (Fig. S2) used. The expected trend that lipids are more effectively extracted with lipophilic solvents such as IPA is primarily, but not always seen for the supernatant (Fig. 3). Using the homogenate in combination with PBS:MeOH (1:1) or PBS:MeOH (1:3) for tissue homogenization and couple it with lipid extraction using 75 % MTBE in MeOH, actually outperforms IPA for lipid as well as polar metabolite extraction.

For polar compounds, however, a small number of organic solvents such as MeOH (50 % and 75 %) or EtOH (85 %) added to PBS seems to provide higher recoveries compared to pure PBS. Here quantitative results seem comparable between homogenate and supernatant, with higher overall recoveries, when using the more lipophilic solution 75 % MTBE in MeOH compared to 25 % MTBE in MeOH for metabolite extraction. Concerning extract volume choice, there seems to be a clear trend towards smaller homogenate volumes for lipids, while for polar metabolites this is only observed for polar homogenization solutions (Fig. S2).

In general, employing the tissue homogenate of PBS:MeOH (1:1) or PBS:MeOH (1:3) in combination with the 2-step metabolite and lipid extraction using 75 % MTBE in MeOH provides overall higher recoveries, but is most efficient for long-chain lipids such as Carn 16:0, LPCa 24:0, PCaa 38:0 and SM 42:1. For the latter, but especially shown for LPC 24:0, the right combination of tissue homogenization and lipid

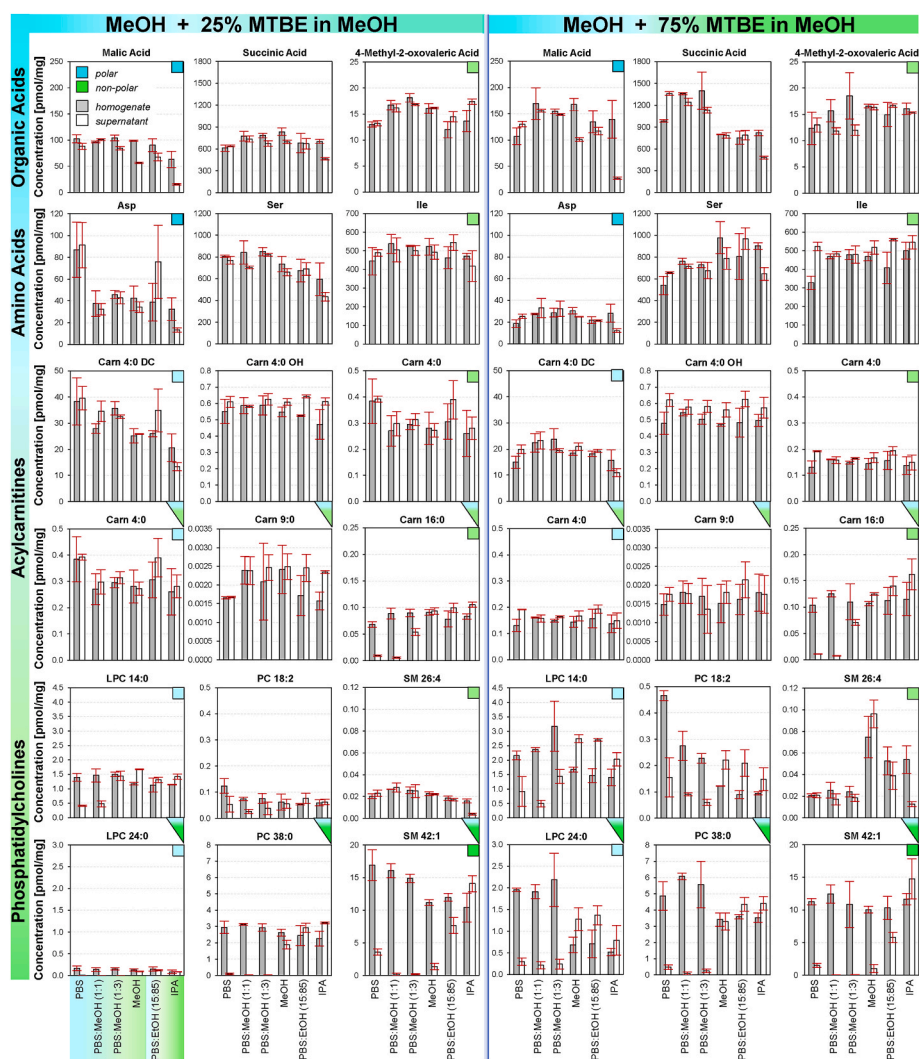


Fig. 3. Bar charts for selected polar metabolite and lipid extraction recoveries for 100 mg pork tissue samples homogenized with 300 μ L PBS, PBS:MeOH (1:1), PBS:MeOH (1:3), MeOH, PBS:EtOH (15:85) or IPA, employing subsequently 50 μ L of homogenate or supernatant, followed by metabolite extraction using 25 % MTBE or 75 % MTBE in MeOH in the second extraction step after MeOH (plus ISTD).

extraction solution employed for tissue homogenates is most important to obtain adequate to high recovery rates. Looking at functional group and alkyl-chain length influence within a small set of acylcarnitines; Carn 4:0 DC, Carn 4:0 OH, Carn 4:0, Carn 9:0 and Carn 16:0, shows for Carn 4:0 DC and Carn 4:0 clearly that PBS in combination with 25 % MTBE in MeOH is preferred to other combinations, while Carn 4:0 OH does not show a preference and the long-chain acylcarnitines require the use of homogenate in combination with 75 % MTBE in MeOH. In case of polar metabolites, Asp, which also carries a free carboxylic acid group, shows a similar trend as Carn 4:0 DC in preferring 25 % MTBE, while the other amino acids such as Ser and Ile provide comparable results for both, 25 % and 75 % MTBE in MeOH (Fig. 3).

In parallel with the tissue homogenization sample preparation, also three different types of blank samples were prepared, in order to determine possible contamination [39,40] from consumables used for tissue homogenization (**Blank 1**), contamination during metabolite and lipid extraction (**Blank 2**) and contaminants introduced by the solvents used and the LC-MS/MS analysis (**Blank 3**). Since **Blank 3** shows the highest contamination levels, possible background contaminations seem to be introduced by solvents and the LC-MS/MS system used (Table S4).

3.4. Comparison of metabolite extraction efficiencies

To evaluate and compare the extraction efficiencies for all quantified metabolites, a 75 % concentration threshold for the highest metabolite concentration is applied to each respective metabolite for all homogenization test solutions, but only for the 50 μ L homogenate and supernatant, extracted with 25 % MTBE and 75 % MTBE, data sets.

The Upset plot in Fig. 4 shows that the best-performing homogenization solutions, in terms of highest extraction recoveries per metabolite and number of metabolites extracted, are PBS:MeOH (1:1), followed by PBS:MeOH (1:3) and PBS, combined with homogenate extraction using 75 % MTBE. Fourth in a row is PBS:EtOH (15:85) for supernatant extraction using 75 % MTBE. The overall worst-performing condition was IPA for tissue homogenization combined with 25 % MTBE for metabolite extraction from the homogenate. This result was most likely caused by the large percentage of solids, generated during homogenization with IPA. As earlier mentioned, such thick clumpy slurries are difficult to pipette, even when using pipette tip pre-wetting and 200 μ L pipette tips. Setting the 75 % concentration threshold for metabolites from the best performing condition, PBS:MeOH (1:1) (Upset plot in Fig. S3 and bar chart in Fig. S4), hence comparing all sample preparation conditions directly to PBS:MeOH (1:1), provides the same best top four conditions, with PBS:MeOH (1:1) with 25 % MTBE for lipid extraction

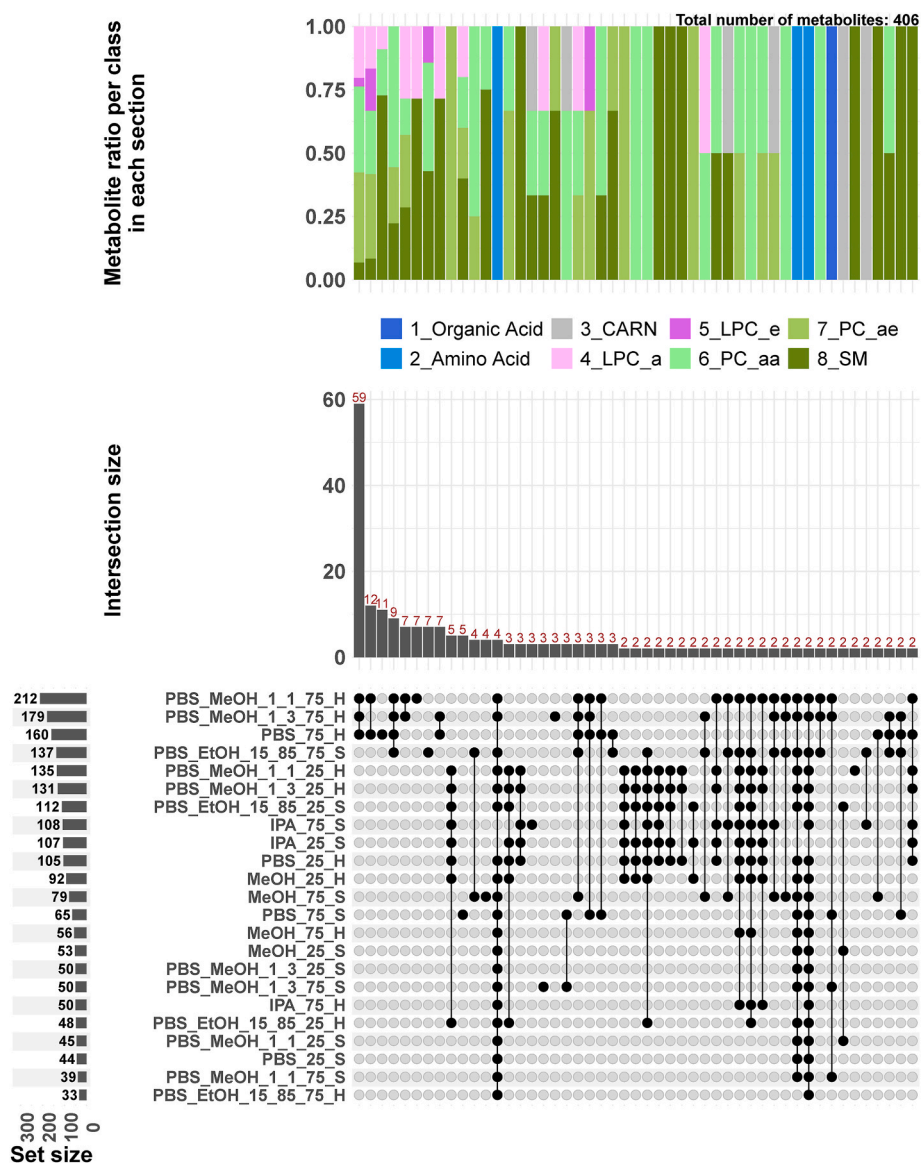


Fig. 4. Upset plot comparing the metabolite extraction recoveries for all investigated homogenization solutions using 50 μ L homogenate (H) and supernatant (S) for metabolite and lipid extraction using 25 % MTBE (25) and 75 % MTBE (75), but only for metabolites with concentrations above the pre-set 75 % concentration threshold for the highest concentrated metabolite independent of the sample preparation used. The bar chart (top graph) shows the percentage of metabolites per substance group, which are extracted by the sample preparation conditions with connected nodes (bottom graph) and contribute to the intersection size (middle graph). For higher visual clarity, an intersection size cut-off of <2 was introduced.

from supernatant now being the worst possible choice.

Fig. S5 displays the number of metabolites per substance group extracted above a concentration threshold of 100 % for the two best-performing homogenization solutions PBS:MeOH (1:1) and PBS:MeOH (1:3). The layered bar charts for 25 % and 75 % MTBE show that in case of using the supernatant instead of the homogenate, the other homogenization solutions always extract more metabolites, which PBS:MeOH (1:1) and PBS:MeOH (1:3) could not sufficiently extract. The best-performing condition, in terms of the highest number of extracted metabolites (395) combined with the highest extraction coverage is, nonetheless, PBS:MeOH (1:1) for tissue homogenization using the homogenate in combination with the more lipophilic 75 % MTBE in MeOH lipid extraction solution. Note that concentration threshold settings for any of the illustrated plots, Upset or layered bar charts are an arbitrary choice. For comparison, a layered bar chart for 75 % and 100 % thresholds is shown in Fig. S4 and Fig. S5, respectively. A detailed description about how to read Upset plots in comparison to Venn diagrams is provided in Supporting Information.

3.5. Mouse pancreas tissue

Fig. 5 shows the metabolite extraction result for three equal pancreas tissue pieces (A, B, and C; 50 mg \pm 10 mg) per pancreas from three different mice (M-1, M-2, and M-3) using PBS:MeOH (1:1) for homogenization and 50 μ L of the homogenate for lipid extraction using the 75 % MTBE procedure. Due to the small tissue weight, metabolite extractions were performed in quadruplicates (error bars) for single homogenization experiments. In general, error bars are small for the higher concentrated metabolites and increase with decreasing concentration levels of the metabolites.

Note that the three pieces of pancreas tissue per mouse were analyzed in random order, independent of their anatomical location. All quantitative results for tissue samples rely on accurate tissue weighing since intermediate results in μ mol/L are converted to pmol/mg tissue. In addition, mouse M-1 was sacrificed at 17 weeks, while mice M-2 and M-3 were sacrificed at 15 weeks. Besides their minimal age difference and although the mice have the same genetic background, biological

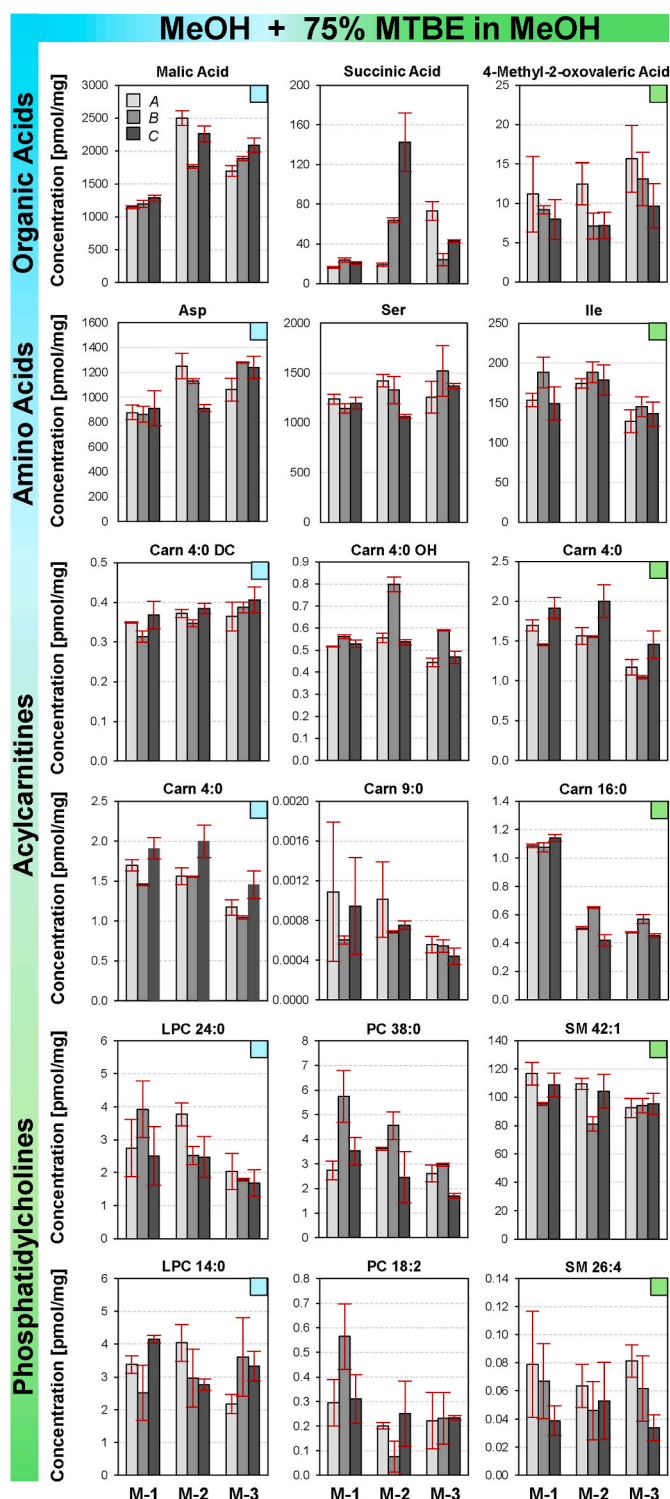


Fig. 5. Bar charts for selected polar metabolite and lipid extraction recoveries of 3 mouse pancreas tissue sections (A, B and C) from three mice (M-1, M-2 and M-3), homogenized with 300 μ L PBS:MeOH (1:1) using five 3 mm steel beads at level 4 for 5 min with ice bag cooling, and employing 50 μ L of the homogenate for metabolite extraction using MeOH and 75 % MTBE in MeOH for polar metabolite and lipid extraction ($n = 4$).

heterogeneity is common in mice and can account for varying metabolite profiles. Moreover, variance of anatomical location might explain the different metabolite profiles of the three tissue pieces from the same mouse, given the differences in blood supply and distribution of

pancreas islets [41]. Malic acid, Carn 16:0, and PC 18:2 show concentration differences between these two age groups, while Carn 4:0 DC does not show significant differences between tissue sections or individual mice. The concentration spike for individual tissue pieces may indicate different metabolic pathway activities for anatomically differently located mouse pancreas tissue sections, while limited research has been reported on this topic, providing a promising avenue for future investigations.

4. Conclusions

The here presented study excerpt resembles the deduction of the best-performing tissue homogenization and metabolite extraction results, concerning comprehensive extraction of polar and highly lipophilic metabolites from tissue samples after comparison of the influence of six different homogenization solutions, employing tissue homogenate and supernatant using three different extract volumes and two different lipid extraction solutions. In total, 60 different conditions were tested with $n = 4$ technical replicates for roughly 400 metabolites and lipids. In context of green analytical chemistry (GAC) [42], only non-halogenated solvents were used throughout this study and solvent waste as well as consumable waste was kept to a minimum by using 96-well plate format for sample preparation and LC-MS/MS analysis, employing only the minimum volumes of solvents and reagents necessary. In addition, the influence of cooling strategy during tissue homogenization was discussed, and a new volume correction factor for homogenate pipetting under prewetting condition, the prewetting correction factor, was introduced. For metabolite and lipid quantification a fully targeted HPLC-ESI-QTRAP-MS/MS metabolomics platform, which comprised four single analysis platforms for amino acid, organic acid, acyl carnitine and phosphocholine lipid quantification (Supporting Information) was employed. In detail, while the homogenization solutions PBS:MeOH (1:1), PBS:MeOH (1:3), and PBS provide better extraction efficiencies for polar metabolites such as amino acids and organic acids, slightly higher extraction efficiencies were revealed, when employing the homogenate instead of the supernatant. Also, lipophilic metabolite recoveries were significantly higher for the homogenate. The use of MeOH or IPA for tissue homogenization mainly improved lipid extraction from the supernatant, but recoveries were nonetheless higher, with higher reproducibility, when adding MeOH to PBS, combined with homogenate extraction using a two-step procedure utilizing MeOH for polar metabolite and 75 % MTBE in MeOH for lipid extraction. It was observed that with increasing organic solvent content, also the number of solids in the homogenate increased, which increased the frequency of pipette tip blockage, making the use of 10 μ L pipette tips without prewetting difficult. In case, 10 μ L pipetting volume in combination with MeOH or IPA is desired (although not recommended by the authors), a prewetting correction factor (PWC-factor) can be employed. Considering that protein in biological samples is removed by precipitation in organic solvents, it can be presumed that the solids in the homogenate comprise cell debris and protein precipitate. Considering the poor extraction efficiency of lipids from the supernatant after centrifugation, it seems obvious that these solids function as an adsorbent, leading to inconsistent results, when employing only the supernatant for metabolite and lipid quantitation. Although lipid extraction recoveries from the supernatant increase, when using higher organic solvent content, the loss of polar metabolites also increases. The decision to separate the homogenization step (300 μ L homogenization solution) from the metabolite extraction step (25 μ L or 50 μ L homogenate), and to furthermore separate the extraction step itself into the subsequent extraction of polar metabolites (450 μ L MeOH) and lipids (450 μ L 75 % MTBE in MeOH) was deliberately made. The volume of homogenization solution is not sufficient to extract all metabolites, and some metabolites simply adhere to solids in the homogenization slurry. Basic liquid-liquid extraction has taught us that larger extraction solvent volumes and an increased number of extraction steps will subsequently increase overall extraction

efficiencies, which in turn increases metabolite coverage and metabolite extraction reproducibility.

Upset plots are a nice tool to compare and visualize extraction efficiencies from big complex data sets [7] compared to Venn-Diagrams [12], which can become challenging to read and understand, when more than 4 data sets are compared. In the here presented study, a multi-dimensional data set generated for 400 metabolites extracted from 24 different sample preparation conditions (shown only for 50 μ L extract volume) was processed. The respective metabolite concentration table in pmol/mg with RSD-% for $n = 4$ or $n = 3$ in case of outlier removal, is provided in the Supporting Information. Conditions which required a prewetting correction are highlighted in yellow. To only compare the high-performing conditions, a concentration threshold of 75 % for the highest metabolite concentration per metabolite was used. The best-performing condition is PBS:MeOH (1:1) using the homogenate for polar metabolite and long-chain lipid extraction using a two-step extraction procedure, employing MeOH for highly polar and 75 % MTBE in MeOH for highly lipophilic metabolites. Nonetheless, different combinations of homogenization solution, homogenization extract type (supernatant or homogenate) and metabolite extraction condition may lead to tissue compartment dependent information. For instance, a homogenization solution low in organic modifier content combined with employing only the homogenization supernatant will most likely mainly show polar cell content metabolites, while the here presented procedure aims to provide a complete polar metabolite and lipid profile of the investigated tissue. Although this study covered a large number of different experimental factors, which influence the generated metabolic profile, the impact of additional parameters such as tissue weight, tissue weight-to-homogenate volume ratio and other factors such as tissue type and different tissue sections of an organ have not yet been fully elucidated. These will be discussed in detail in subsequent research studies. In a short preliminary exploratory study, the metabolite profiles of nine pancreas tissue sections from three individual mice were investigated, revealing that metabolic profiles are highly dependent on the specific anatomical position of pancreas tissue sections of healthy mice.

CRedit authorship contribution statement

Yuntao Hao: Writing – review & editing, Writing – original draft, Visualization, Validation, Software, Investigation, Formal analysis, Data curation. **Jeannie Horak:** Writing – review & editing, Writing – original draft, Visualization, Validation, Supervision, Software, Project administration, Methodology, Investigation, Formal analysis, Data curation, Conceptualization. **Zorica Stijepic:** Writing – review & editing, Validation, Methodology, Investigation. **Sultan Nilay Can:** Writing – review & editing, Software, Formal analysis. **Luke Tu:** Software, Validation, Writing – review & editing. **Julia Alexandra Wolff:** Writing – review & editing, Resources. **Berthold Koletzko:** Writing – review & editing, Resources, Funding acquisition.

Ethical statement

Three mice used for methodological application were not included in any experiments and were sacrificed only for organ isolation, which is permitted by the §4 of the German Animal Welfare Act (Tierschutzgesetz) and hence no ethical approval was needed.

Funding

Yuntao Hao is the recipient of a fellowship granted by the Chinese Scholarship Council (CSC) [No. 202006010048, 2020]. Luke Tu is the recipient of a fellowship granted by the Hans-Böckler Stiftung (HBS) [414094, 2022]. This work was financially supported in part by the German Center for Child and Adolescent Health (DZKJ) [01GL2406A, 2024]. Berthold Koletzko is the Else Kröner Seniorprofessor of Paediatrics at LMU – University of Munich, financially supported by the

charitable Else Kröner-Fresenius-Foundation (EKfz), LMU Medical Faculty and LMU University Hospitals [No. 2020_EKSP.119, 2020].

Declaration of competing interest

The authors declare no conflict of interest. The CSC, HBS, EKfz and DZKJ funding organizations were not involved in the study design, its outcome, or the writing of this article.

Acknowledgements

The authors thank Stephanie-Katrin Magdalena Winterstetter for HPLC-ESI-QTRAP-MS/MS analysis and quantitative data evaluation.

Appendix. ASupplementary data

Supplementary data to this article can be found online at <https://doi.org/10.1016/j.aca.2025.343728>.

Data availability

Data will be made available on request.

References

- [1] A.M. Jones, M.T. Van de Wyngaerde, E.T. Machtinger, E.G. Rajotte, T.C. Baker, Choice of laboratory tissue homogenizers matters when recovering nucleic acid from medically important ticks, *J. Med. Entomol.* 57 (4) (2020) 1221–1227, <https://doi.org/10.1093/jme/tjaa006>.
- [2] Y. Gao, X. Zhao, sncRiboTag-Seq: cell-type-specific RiboTag-Seq for cells in low abundance in mouse brain tissue, *STAR Protoc* 2 (1) (2021) 100231, <https://doi.org/10.1016/j.xpro.2020.100231>.
- [3] A.A. Karpinski, J.C. Torres Elguera, A. Sanner, W. Konopka, L. Kaczmarek, D. Winter, A. Konopka, E. Bulska, Study on tissue homogenization buffer composition for brain mass spectrometry-based proteomics, *Biomedicines* 10 (10) (2022) 2466, <https://doi.org/10.3390/biomedicines10102466>.
- [4] P.B. Naidu, P. Ponnuragan, M.S. Begum, K. Mohan, B. Meriga, R. RavindarNaik, G. Saravanan, Diosgenin reorganises hyperglycaemia and distorted tissue lipid profile in high-fat diet-streptozotocin-induced diabetic rats, *J. Sci. Food Agric.* 95 (15) (2015) 3177–3182, <https://doi.org/10.1002/jsfa.7057>.
- [5] J.M. Berg, J.L. Tymoczko, L. Stryer, Each organ has a unique metabolic profile. *Biochemistry*, W. H. Freeman, New York, 2006, pp. 851–854.
- [6] K. Kishida, N. Furusawa, Simultaneous determination of sulfamonomethoxine, sulfadimethoxine, and their hydroxy/N 4-acetyl metabolites with gradient liquid chromatography in chicken plasma, tissues, and eggs, *Talanta* 67 (1) (2005) 54–58, <https://doi.org/10.1016/j.talanta.2005.02.005>.
- [7] B. Wanciewicz, M.R. Pergande, Y. Zhu, Z. Gao, Z. Shi, K. Plouff, Y. Ge, Comprehensive metabolomic analysis of human heart tissue enabled by parallel metabolite extraction and high-resolution mass spectrometry, *Anal. Chem.* 96 (15) (2024) 5781–5789, <https://doi.org/10.1021/acs.analchem.3c04353>. Washington, DC, U. S.
- [8] S.W. Gooding, M.A. Chrenek, S. Ferdous, J.M. Nickerson, J.H. Boatright, Set screw homogenization of murine ocular tissue, including the whole eye, *Mol. Vision* 24 (2018) 690–699.
- [9] M. Hoering, S. Krautbauer, L. Hiltl, V. Babl, A. Sigrüener, R. Burkhardt, G. Liebisch, Accurate lipid quantification of tissue homogenates requires suitable sample concentration, solvent composition, and homogenization procedure—a case study in murine liver, *Metabolites* 11 (6) (2021) 365, <https://doi.org/10.3390/metabo11060365>.
- [10] C. Andresen, T. Boch, H.M. Gegner, N. Mechtel, A. Narr, E. Birgin, E. Rasbach, N. Rahbari, A. Trumpp, G. Poschet, D. Huebschmann, Comparison of extraction methods for intracellular metabolomics of human tissues, *Front. Mol. Biosci.* 9 (2022) 932261, <https://doi.org/10.3389/fmolb.2022.932261>.
- [11] S. Redanz, A. Podbielski, P. Warnke, Improved microbiological diagnostic due to utilization of a high-throughput homogenizer for routine tissue processing, *Diagn. Microbiol. Infect. Dis.* 82 (3) (2015) 189–193, <https://doi.org/10.1016/j.diagmicrobio.2015.03.018>.
- [12] P. Cuevas-Delgado, N. Warmuzinska, K. Luczykowski, B. Bojko, C. Barbas, Exploring sample treatment strategies for untargeted metabolomics: a comparative study of solid phase microextraction (SPME) and homogenization with solid-liquid extraction (SLE) in renal tissue, *Anal. Chim. Acta* 1312 (2024) 342758, <https://doi.org/10.1016/j.aca.2024.342758>.
- [13] D.B. Dias, R. Fritsche-Guenther, F. Gutmann, G.N. Duda, J. Kirwan, P.S.P. Poh, A comparison of solvent-based extraction methods to assess the central carbon metabolites in mouse bone and muscle, *Metabolites* 12 (5) (2022) 453, <https://doi.org/10.3390/metabo12050453>.
- [14] J. Balog, L. Sasi-Szabo, J. Kinross, M.R. Lewis, L.J. Muirhead, K. Veselkov, R. Mirnezami, B. Dezso, L. Damjanovich, A. Darzi, J.K. Nicholson, Z. Takats,

- Intraoperative tissue identification using rapid evaporative ionization mass spectrometry, *Sci. Transl. Med.* 5 (194) (2013) 112, <https://doi.org/10.1126/scitranslmed.3005623>, 194ra193.
- [15] E. Manoli, S. Mason, L. Ford, A. Adebesein, Z. Bodai, A. Darzi, J. Kinross, Z. Takats, Validation of ultrasonic harmonic scalpel for real-time tissue identification using rapid evaporative ionization mass spectrometry, *Anal. Chem.* (Washington, DC, U. S.) 93 (14) (2021) 5906–5916, <https://doi.org/10.1021/acs.analchem.1c00270>.
- [16] M. Stoeckli, P. Chaurand, D.E. Hallahan, R.M. Caprioli, Imaging mass spectrometry: a new technology for the analysis of protein expression in mammalian tissues, *Nat. Med.* (N. Y., NY, U. S.) 7 (4) (2001) 493–496, <https://doi.org/10.1038/86573>.
- [17] C. Sun, A. Wang, Y. Zhou, P. Chen, X. Wang, J. Huang, J. Gao, X. Wang, L. Shu, J. Lu, W. Dai, Z. Bu, J. Ji, J. He, Spatially resolved multi-omics highlights cell-specific metabolic remodeling and interactions in gastric cancer, *Nat. Commun.* 14 (1) (2023) 2692, <https://doi.org/10.1038/s41467-023-38360-5>.
- [18] F. Li, R. Karongo, D. Mavridou, J. Horak, A. Sievers-Engler, M. Laemmerhofer, Automated sample preparation with 6-Aminoquinolyl-N-hydroxysuccinimidyl carbamate and iodoacetamide derivatization reagents for enantioselective liquid chromatography tandem mass spectrometry amino acid analysis, *J. Chromatogr. A* 1708 (2023) 464349, <https://doi.org/10.1016/j.chroma.2023.464349>.
- [19] E.G. Bligh, W.J. Dyer, A rapid method of total lipid extraction and purification. FIELD Authors:BLIGH, E G; DYER, W J, *Can. J. Biochem. Physiol.* 37 (8) (1959) 911–917, <https://doi.org/10.1139/o59-099>.
- [20] C. Calderon, C. Sanwald, J. Schlotterbeck, B. Drotleff, M. Laemmerhofer, Comparison of simple monophasic versus classical biphasic extraction protocols for comprehensive UHPLC-MS/MS lipidomic analysis of HeLa cells, *Anal. Chim. Acta* 1048 (2019) 66–74, <https://doi.org/10.1016/j.aca.2018.10.035>.
- [21] H.M. Gegner, N. Mechtel, E. Heidenreich, A. Wirth, F.G. Cortizo, K. Bennewitz, T. Fleming, C. Andresen, M. Freichel, A.A. Teleman, J. Kroll, R. Hell, G. Poschet, Deep metabolic profiling assessment of tissue extraction protocols for three model organisms, *Front. Chem.* 10 (2022) 869732, <https://doi.org/10.3389/fchem.2022.869732>.
- [22] S. Zukunft, C. Pohn, C. Roehring, G. Moeller, M. Hrabe de Angelis, J. Adamski, J. Tokarz, High-throughput extraction and quantification method for targeted metabolomics in murine tissues, *Metabolomics* 14 (1) (2018) 1–12, <https://doi.org/10.1007/s11306-017-1312-x>.
- [23] T. Boegl, F. Mlynek, M. Himmelsbach, W. Buchberger, Comparison of one-phase and two-phase extraction methods for porcine tissue lipidomics applying a fast and reliable tentative annotation workflow, *Talanta* 236 (2022) 122849, <https://doi.org/10.1016/j.talanta.2021.122849>.
- [24] E. Dorochow, R. Gurke, S. Rischke, G. Geisslinger, L. Hahnefeld, Effects of different storage conditions on lipid stability in mice tissue homogenates, *Metabolites* 13 (4) (2023) 504, <https://doi.org/10.3390/metabo13040504>.
- [25] R.W. Jiang, K. Jaroch, J. Pawliszyn, Solid-phase microextraction of endogenous metabolites from intact tissue validated using a Biocrates standard reference method kit, FIELD Authors:Jiang, Runshan Will; Jaroch, Karol; Pawliszyn, Janusz, *J. Pharm. Anal.* 13 (1) (2023) 55–62, <https://doi.org/10.1016/j.jppha.2022.09.002>.
- [26] S. Ayache, M. Panelli, F.M. Marincola, D.F. Stroneck, Effects of storage time and exogenous protease inhibitors on plasma protein levels, *Am. J. Clin. Pathol.* 126 (2) (2006) 174–184, <https://doi.org/10.1309/3wm7xj7rd8bclnkx>.
- [27] M. Schwaiger-Haber, E. Stancliffe, V. Arends, B. Thyagarajan, M. Sindelar, G. J. Patti, A workflow to perform targeted metabolomics at the untargeted scale on a triple quadrupole mass spectrometer, *ACS Meas. Sci. Au* 1 (1) (2021) 35–45, <https://doi.org/10.1021/acsmesuresciau.1c00007>.
- [28] A. Sens, S. Rischke, L. Hahnefeld, E. Dorochow, S.M.G. Schaefer, D. Thomas, M. Koehm, G. Geisslinger, F. Behrens, R. Gurke, Pre-analytical sample handling standardization for reliable measurement of metabolites and lipids in LC-MS-based clinical research, *J. Mass Spectrom. Adv. Clin. Lab* 28 (2023) 35–46, <https://doi.org/10.1016/j.jmsacl.2023.02.002>.
- [29] C.E. Ramsden, Z.-X. Yuan, M.S. Horowitz, D. Zamora, S.F. Majchrzak-Hong, B. S. Muhlhauser, A.Y. Taha, M. Makrides, R.A. Gibson, Temperature and time-dependent effects of delayed blood processing on oxylipin concentrations in human plasma, *Prostaglandins, Leukotrienes Essent. Fatty Acids* 150 (2019) 31–37, <https://doi.org/10.1016/j.plefa.2019.09.001>.
- [30] K.L. Lindsay, C. Hellmuth, O. Uhl, C. Buss, P.D. Wadhwa, B. Koletzko, S. Entinger, Longitudinal metabolomic profiling of amino acids and lipids across healthy pregnancy, *PLoS One* 10 (12) (2015) e0145794, <https://doi.org/10.1371/journal.pone.0145794>, 0145791-e0145794/0145791.
- [31] High-throughput drug stability assessment via biomimetic metalloporphyrin-catalyzed reactions using laser-assisted rapid evaporative ionization mass spectrometry (LA-REIMS). FIELD authors:marion, andrás; mohácsi, zombor; decsi, balázs; csillag, balázs; balog, júlia; schäffer, richard; karancsi, tamás; balogh, györgy tiber, *Pharmaceutics* 16 (10) (2024), <https://doi.org/10.3390/pharmaceutics16101266>.
- [32] U. Harder, B. Koletzko, W. Peissner, Quantification of 22 plasma amino acids combining derivatization and ion-pair LC-MS/MS, *J. Chromatogr., B: Anal. Technol. Biomed. Life Sci.* 879 (7–8) (2011) 495–504, <https://doi.org/10.1016/j.jchromb.2011.01.010>.
- [33] E. Newton-Tanzer, H. Demmelmaier, J. Horak, L. Holdt, B. Koletzko, V. Grote, Acute metabolic response in adults to toddler milk formulas with alternating higher and lower protein and fat contents, a randomized cross-over trial, *Nutrients* 13 (9) (2021) 3022, <https://doi.org/10.3390/nu13093022>.
- [34] P. Giesbertz, J. Ecker, A. Haag, B. Spanier, H. Daniel, An LC-MS/MS method to quantify acylcarnitine species including isomeric and odd-numbered forms in plasma and tissues, *J. Lipid Res.* 56 (10) (2015) 2029–2039, <https://doi.org/10.1194/jlr.D061721>.
- [35] J. Marques, E. Shokry, O. Uhl, L. Baber, F. Hofmeister, S. Jarmusch, M. Bidlingmaier, U. Ferrari, B. Koletzko, M. Drey, Sarcopenia: investigation of metabolic changes and its associated mechanisms, *Skeletal Muscle* 13 (1) (2023) 2, <https://doi.org/10.1186/s13395-022-00312-w>.
- [36] S. Rauschert, O. Uhl, B. Koletzko, F. Kirchberg, T.A. Mori, R.-C. Huang, L.J. Beilin, C. Hellmuth, W.H. Oddy, Lipidomics reveals associations of phospholipids with obesity and insulin resistance in young adults, *J. Clin. Endocrinol. Metab.* 101 (3) (2016) 871–879, <https://doi.org/10.1210/jc.2015-3525>.
- [37] J.R. Conway, A. Lex, N. Gehlenborg, UpSetR: An R package for the visualization of intersecting sets and their properties, *Bioinformatics* 33 (18) (2017) 2938–2940, <https://doi.org/10.1093/bioinformatics/btx364>.
- [38] M. Krassowski, ComplexUpset 1.3.5. https://krassowski.github.io/complex-upset/articles/Examples_R.html, 2020. (Accessed 4 June 2024).
- [39] S. Sofalvi, E.S. Lavins, C.K. Kaspar, H.M. Michel, C.L. Mitchell-Mata, M.A. Huestis, L.G. Apollonio, Development and validation of an LC-MS-MS method for the detection of 40 benzodiazepines and three Z-drugs in blood and urine by solid-phase extraction, *J. Anal. Toxicol.* 44 (7) (2020) 708–717, <https://doi.org/10.1093/jat/bkaa072>.
- [40] S.P. Maputla, W. Van Dalen, A. Joubert, J. Norman, S. Castel, M. van der Merwe, L. Wiesner, A validated liquid chromatography-tandem mass spectrometry assay for the analysis of isoniazid and its metabolite acetyl-isoniazid in urine, *J. Mass Spectrom. Adv. Clin. Lab* 32 (2024) 11–17, <https://doi.org/10.1016/j.jmsacl.2024.02.001>.
- [41] J. Dolensek, M.S. Rupnik, A. Stožer, Structural similarities and differences between the human and the mouse pancreas. FIELD authors:dolensek, jurij; rupnik, marjan slak; stožer, andraž, *Islets* 7 (1) (2015) e1024405 <https://doi.org/10.1080/19382014.2015.1024405>.
- [42] A. Gatuszka, Z. Migaszewski, J. Namieśnik, TrAC Trends Anal. Chem. 50 (2013) 78–84, <https://doi.org/10.1016/j.trac.2013.04.010>.